Critical behaviour and interfacial fluctuations in a phase-separating model colloid–polymer mixture: grand canonical Monte Carlo simulations

2004 J. Phys.: Condens. Matter 16 S3807

(http://iopscience.iop.org/0953-8984/16/38/003)

INSTITUTE OF PHYSICS PUBLISHING JOURNAL OF PHYSICS: CONDENSED MATTER

J. Phys.: Condens. Matter **16** (2004) S3807–S3820 PII: S0953-8984(04)78576-8

Critical behaviour and interfacial fluctuations in a phase-separating model colloid–polymer mixture: grand canonical Monte Carlo simulations

R L C Vink and J Horbach

Institut für Physik, Johannes Gutenberg-Universität, D-55099 Mainz, Staudinger Weg 7, Germany

Received 29 March 2004
Published 10 September 2004
Online at stacks.iop.org/JPhysCM/16/S3807
doi:10.1088/0953-8984/16/38/003

Abstract

By using Monte Carlo simulations in the grand canonical ensemble we investigate the bulk phase behaviour of a model colloid–polymer mixture, the so-called Asakura–Oosawa model. In this model the colloids and polymers are considered as spheres with a hard-sphere colloid–colloid and colloid–polymer interaction and a zero interaction between polymers. In order to circumvent the problem of low acceptance rates for colloid insertions, we introduce a cluster move where a cluster of polymers is replaced by a colloid. We consider the transition from a colloid-poor to colloid-rich phase which is analogous to the gas–liquid transition in simple liquids. Successive umbrella sampling, recently introduced by Virnau and Müller (2003 *Preprint* cond-mat/0306678), is used to access the phase-separated regime. We calculate the demixing binodal and the interfacial tension, also in the region close to the critical point. Finite size scaling techniques are used to accurately locate the critical point. Also investigated are the colloid density profiles in the phase-separated regime. We extract the interfacial thickness w from the latter profiles and demonstrate that the interfaces are subject to spatial fluctuations that can be understood by capillary wave theory. In particular, we find that, as predicted by capillary wave theory, w^2 diverges logarithmically with the size of the system parallel to the interface.

1. Introduction

Mixtures of colloids and non-adsorbing polymers continue to be an exciting meeting ground for experimental, theoretical and computer simulation research. It is known from experiments (e.g. [1, 2]) that these systems may exhibit a fluid–fluid phase-separation of purely entropic origin which is due to a depletion effect. According to this, in a colloid–polymer mixture, each colloidal particle is surrounded by a depletion zone from which polymers are excluded. When two colloids are close together, their depletion zones may overlap, thereby increasing

the free volume, and hence the entropy, of the polymers. If the gain in entropy is sufficient, demixing will occur. The demixing transition is thus of profound theoretical interest because it is driven by entropy, and not by energy. From an experimental point of view, colloid–polymer mixtures are moreover interesting since, because of the relatively large size of the particles, very detailed information can be obtained. In the case of a phase-separated mixture, it is even possible to directly observe the colloid–polymer interface [3]. Very recently, Aarts *et al* [4] were even able to visualize experimentally capillary waves, i.e. spatial fluctuations of the colloid–polymer interface.

Colloid–polymer mixtures are thus convenient model systems to study a range of physical phenomena. As a result, these mixtures have sparked many experimental and theoretical investigations, and also computer simulations. On the theoretical side, much progress was made with the colloid–polymer model introduced by Asakura and Oosawa [5, 6]. In this model (the AO model) colloids and polymers are treated as spheres with respective radii R_c and R_p. Hard sphere interactions are assumed between colloid–colloid (cc) and colloid–polymer (cp) pairs, while polymer–polymer (pp) pairs can interpenetrate freely. This yields the following pair potentials:

$$\begin{aligned} u_{cc}(r) &= \begin{cases} \infty & \text{for } r < 2R_c \\ 0 & \text{otherwise,} \end{cases} \\ u_{cp}(r) &= \begin{cases} \infty & \text{for } r < R_c + R_p \\ 0 & \text{otherwise,} \end{cases} \\ u_{pp}(r) &= 0, \end{aligned} \tag{1}$$

where r is the distance between two particles. The polymers thus represent ideal polymer coils with a radius of gyration R_p.

Much insight into the phase behaviour of the AO model was gained using the free volume method of Lekkerkerker [7] (in [8] this approach was also applied to interacting polymers). This method was used to obtain the phase diagram for a wide range of colloid to polymer size ratios $q \equiv R_p/R_c$ on a mean-field level. The general result is that demixing occurs for $q \approx 0.25$ and above, provided that the polymer fugacity is high enough. Additional progress was made with density functional theory (DFT). DFT was used to estimate the interfacial tension of the colloid–polymer interface, and also the colloid density profile across the interface, but again on a mean-field level [9, 10].

Many of the theoretical predictions for the AO model have been tested in computer simulations [11–14]. In general, these simulations yield binodals in reasonable agreement with mean-field free volume theory. Unfortunately, close to the critical point, precisely in the regime where mean-field approximations are expected to break down, these simulations suffer from large error bars. This is especially true for simulations carried out in the Gibbs ensemble. Thus, a meaningful comparison between theory and simulation is not possible in the vicinity of the critical point by means of the latter MC simulations. However, note that in [12, 14] fluid–solid binodals were also presented.

Recently, we introduced a Monte Carlo (MC) method that enables us to simulate the AO model in the grand canonical ensemble [15, 16]. The grand canonical ensemble naturally lends itself to the study of phase separation, and offers a number of advantages over the canonical and the Gibbs ensemble. On the one hand, it allows for accurate measurements of the binodal, also in the region close to the critical point. On the other hand, it can be used to study interfacial properties (interfacial tension, density profiles) in the case of phase-separated mixtures.

The purpose of this paper is two-fold. First, we show in which regime mean-field approximations for the AO model are reliable. To this end, we use our method to obtain

the phase diagram of the AO model, and compare it directly to the free volume result. As it turns out, the deviations become substantial close to the critical point. This is to be expected though, because the AO model belongs to the 3D Ising universality class. We then present an accurate estimate of the critical point using finite size scaling techniques. Second, we quantify the effects of capillary waves on the width of the colloid–polymer interface in a phase-separated AO mixture. Although these effects are often ignored (an exception is the nice review article of Brader *et al* [17]), our results for the AO model indicate that interface broadening is an important effect.

The outline of this paper is as follows. In section 2 we present the used simulation methods and the phase diagram followed by the results of finite size scaling to estimate the critical point (section 3). Next, we discuss the effects of capillary waves (section 4). We end with a number of conclusions in section 5.

2. Phase diagram and interfacial tension

In order to study the phase behaviour of the AO model we use MC simulations in the grand canonical ensemble, in which the volume V, the respective fugacities $\{z_c, z_p\}$ of colloids and polymers, and the temperature T are fixed [18]. Note that the number of particles inside V is a fluctuating quantity in the grand canonical ensemble. Since in the AO model all allowed configurations have zero potential energy, temperature plays a trivial role and the phase behaviour is controlled by the colloid to polymer size ratio q and the fugacities $\{z_c, z_p\}$. We consider here a size ratio $q = 0.8$ and put $R_c \equiv 1$ to set the length scale. The simulations are performed in a box with edges $L_x \times L_y \times L_z$ using periodic boundary conditions. One defines the quantity $\eta_p^r \equiv z_p(4\pi/3)R_p^3$, known as the polymer reservoir packing fraction, which plays a role similar to the inverse temperature in simple fluids (e.g. the Lennard-Jones model).

The use of the grand canonical ensemble allows one to bypass certain problems encountered in the canonical or the Gibbs ensemble. As we shall see below, it remains efficient close to the critical point, and it allows for an accurate determination of the interfacial tension. Moreover, the machinery of finite-size scaling can readily be applied in the grand canonical ensemble. The difficulty of inserting a colloid into a dense polymer system is alleviated by using a cluster move. The main idea of this MC move is to not insert and remove particles one at a time, but to remove a cluster of polymers for each colloid that is inserted. The details of this move are provided elsewhere [15, 16]. A reweighting scheme enables the simulation to cross the free energy barrier separating the colloid vapour phase from the colloid liquid phase, and sample the phase-separated regime. Many reweighting schemes are available [18, 19]. We use the recently developed *successive umbrella sampling*, the details of which can be found in the original reference [20].

We demonstrate now that the grand canonical MC in conjunction with the aforementioned cluster move and successive umbrella sampling is well-suited to determine the binodal and properties of the interface between the phase-separated species such as the interfacial tension. During the simulation, one measures the probability $P(\eta_c)$ that a certain colloid packing fraction $\eta_c \equiv (4\pi/3)R_c^3 N_c/V$ is observed in a simulation box of fixed volume V (N_c is the total number of colloids inside V), i.e. one maintains a histogram counting how often a certain colloid packing fraction has occurred. Two different system sizes are considered in this section: $V_1 = (L_x = L_y = 13.3; L_z = 26.5)$ and $V_2 = (L_x = L_y = 16.7; L_z = 33.4)$, where the colloid radius R_c was taken to be the unit of length. Note that the use of elongated simulation boxes is important for the determination of the interfacial tension (see below). More details on the simulation can be found elsewhere [15, 16].

If a phase separation occurs, $P(\eta_c)$ is bimodal. A number of example distributions for this case are shown in figure 1. The peaks at low η_c correspond to the colloid vapour phase and those

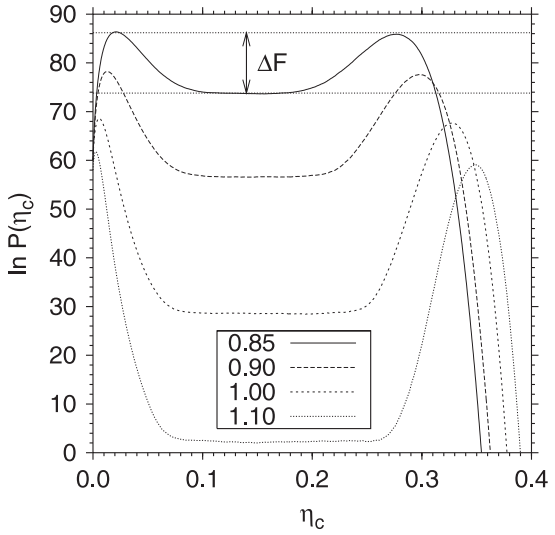

Figure 1. Logarithm of the probability $P(\eta_c)$ of observing a colloid packing fraction η_c for an AO mixture with $q = 0.8$ at coexistence for several values of η_p^r as indicated. The simulations were performed in a box with dimensions $L_x = L_y = 16.7$ and $L_z = 33.4$ using periodic boundary conditions. Note that the distributions are not normalized.

at high η_c to the colloid liquid phase. The region in between is the phase-separated regime. The distributions in figure 1 were obtained at coexistence, which means that the fugacity z_c was tuned such that the area under both peaks is equal. The height of the barrier marked ΔF in figure 1 corresponds to the free energy barrier separating the coexisting phases. As was shown by Binder [21], this barrier is related to the interfacial tension via $\gamma = \Delta F/(2A)$ (with $A = L_x \cdot L_y$ the area of the interface) provided that the size of the system is large enough. The factor $1/2$ in the latter equation for γ stems from the use of periodic boundary conditions that yield to the formation of two interfaces in the system. It is crucial to use an elongated box for an accurate determination of γ since this enforces the flat region seen in the distributions $P(\eta_c)$ which indicate that the two interfaces in the phase-separated regime are well-separated from each other and thus interactions between the interfaces are suppressed.

It is also interesting to measure the average polymer packing fraction $\eta_p \equiv (4\pi/3)R_p^3 N_p/V$ as a function of η_c, with N_p being the number of polymers inside V. This result is shown in figure 2. In the pure polymer phase ($\eta_c = 0$) we expect $\eta_p = \eta_p^r$ because the polymers then form an ideal gas. This is precisely what figure 2 shows: as the colloid packing fraction in the system increases, the polymer packing fraction in the system decreases and it is almost zero at $\eta_c = 0.4$.

As already mentioned, η_p^r is the control parameter in the AO model, much like temperature is for the fluid–vapour transition in molecular systems. To obtain the phase diagram, one simply measures $P(\eta_c)$ at coexistence for a number of different η_p^r. For each $P(\eta_c)$ at coexistence, one reads off the colloid packing fraction of the vapour phase η_c^V and of the liquid phase η_c^L. This yields the phase diagram in reservoir representation, shown in the inset of figure 3. By using the result of figure 2 we can convert the reservoir representation into the experimentally more relevant $\{\eta_c, \eta_p\}$ or system representation, also shown in figure 3. For each $P(\eta_c)$, one additionally obtains a value for the interfacial tension using the method of Binder. The results of this procedure are shown in figure 4, in two different representations.

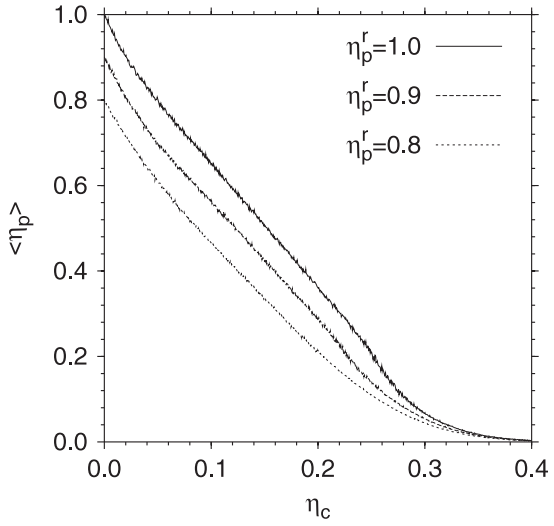

Figure 2. Average polymer packing fraction $\langle \eta_p \rangle$ as a function of the colloid packing fraction η_c for an AO mixture with $q = 0.8$ and various values for η_p^r as indicated.

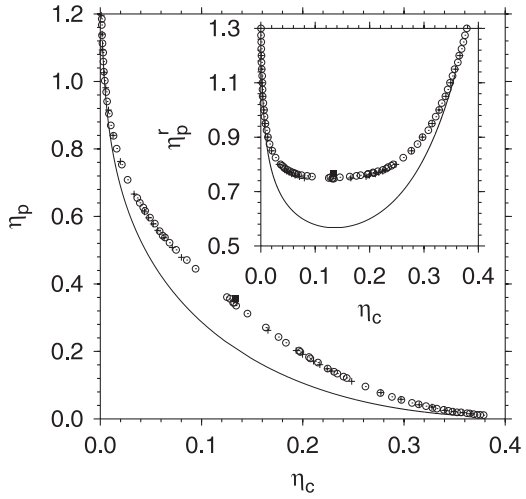

Figure 3. Phase diagram of the AO model with $q = 0.8$ in system representation. Open circles were obtained using box dimensions $L_x = L_y = 16.7$ and $L_z = 33.4$; crosses were obtained in a smaller box with dimensions $L_x = L_y = 13.3$ and $L_z = 26.5$. The inset shows the phase diagram in reservoir representation. The squares mark the location of the critical point as obtained using finite size scaling. The solid curves are results from free volume theory [7, 8].

Comparison of the simulation results in figure 3 shows that finite-size effects are relatively small, even close to the critical point. However, substantial deviations from free volume theory are visible, especially in the region close to the critical point. Free volume theory underestimates the critical polymer fugacity by about 30%. More importantly, this theory yields the typical mean-field parabolic shape of the binodal (critical exponent $\beta = 1/2$) while in the simulation one obtains the expected flatter binodal. The latter is compatible with a critical exponent $\beta \approx 0.325$, corresponding to the 3D Ising universality class [22].

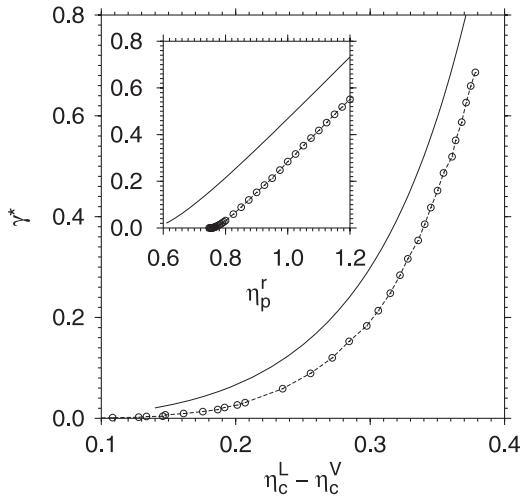

Figure 4. Reduced interfacial tension $\gamma^* \equiv 4R_c^2\gamma/(k_BT)$ for an AO mixture with $q = 0.8$ as a function of the difference in packing fraction between the coexisting phases. The box dimensions are $L_x = L_y = 16.7$ and $L_z = 33.4$. The inset shows γ^* as a function of η_p^r. Open circles are simulation results; the solid curves are DFT results using fundamental measure theory [23].

In figure 4, the reduced interfacial tension $\gamma^* \equiv 4R_c^2\gamma$ is shown as a function of η_p^r (inset) and as a function of the difference in the colloid packing fractions of the liquid (L) and the vapour (V) phase at coexistence, η_c^L–η_c^V. Also included in the figure is the result from a recent DFT [23]. Although the DFT overestimates the interfacial tension as determined from the simulation by about 30%, the qualitative behaviour is very similar: both methods predict a sharp increase in the interfacial tension as η_p^r increases. Note that experimental data for γ^* are of the same order as those obtained from simulation and DFT [1, 2]. However, in order to describe colloid–polymer mixtures on a quantitative level, more sophisticated models than the AO model are required.

3. Finite size scaling

In this section we determine the critical values of the polymer fugacity $\eta_{p,cr}^r$, the colloid chemical potential $\mu_{c,cr} \equiv k_BT\ln(z_{c,cr})$ (with k_B the Boltzmann constant), the polymer packing fraction $\eta_{p,cr}$, and the colloid packing fraction $\eta_{c,cr}$, by using finite size scaling (FSS) techniques. FSS is readily applicable to grand canonical MC [24]. The great advantage in this case is that the total number of particles is allowed to fluctuate. Therefore, the critical order-parameter fluctuations can be observed on the maximum length scale possible, namely the system size itself.

The standard approach is to measure the cumulant ratio of the probability distribution $P(\eta_c)$ as a function of the control parameter for different system sizes. As shown by Binder [25], the cumulant becomes system size independent at the critical value of the control parameter provided that the system is large enough such that corrections to FSS are negligible. To locate the critical point, we thus need to measure the value of (for example) the first order cumulant $M = \langle m^2\rangle/\langle|m|\rangle^2$ as a function of η_p^r close to the critical point for different system sizes, with $m = \eta_c - \langle\eta_c\rangle$. The results of this procedure are shown in figure 5. Note that the simulations were done in cubic simulation boxes with different lengths L, the values of which are indicated in figure 5. The critical fugacity is at the intersection of the lines, from which we obtain $\eta_{p,cr}^r = 0.766 \pm 0.002$.

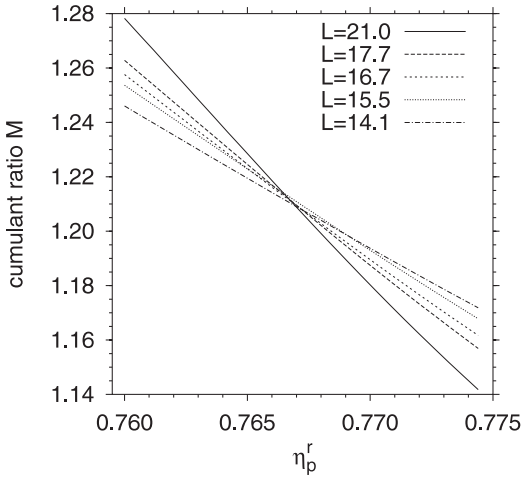

Figure 5. Cumulant ratio M as a function of η_p^r for an AO mixture with $q = 0.8$ for various system sizes. The simulations were performed in a cubic box with length L as indicated. From the intercept we obtain for the critical polymer fugacity $\eta_{p,cr}^r = 0.766 \pm 0.002$.

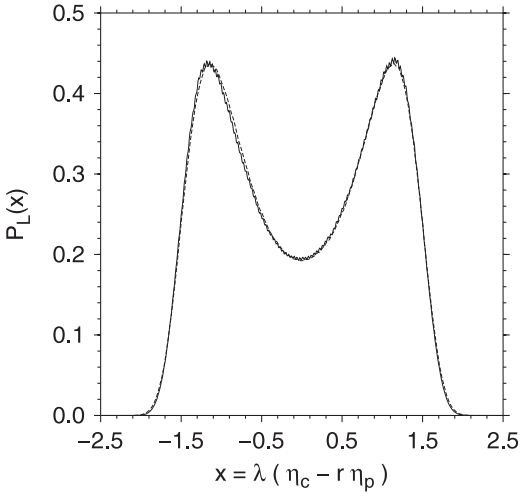

Figure 6. Collapse of a measured AO model probability distribution onto the 3D Ising fixed point function. The solid curve is the measured form of $P(\eta_c - r\eta_p)$ for an AO model with $q = 0.8$ and $r = 0.25$ in a cubic box with edge $L = 21.0$ and $\eta_p^r = 0.7645$. The dashed curve is the universal fixed point function for the 3D Ising model [27]. The parameter λ is chosen such that both distributions have unit variance.

Systems having short ranged interactions and a single component order parameter, such as the AO model, are expected to belong to the 3D Ising universality class [26]. This means that their scaling functions and critical exponents are identical to those of the 3D Ising model. Consequently, the probability distribution $P(\eta_c)$ for the AO model at criticality must match the universal fixed point function $P_L(x)$ appropriate to the 3D Ising model. The latter function is known from independent studies of the Ising model [27], and is shown in figure 6. $P_L(x)$ can be used to locate critical values, in that one finds for instance the apparent polymer fugacity η_p^{r*} for which $P(\eta_c)$ collapses onto $P_L(x)$. Since $P_L(x)$ is symmetric around the origin, and $P(\eta_c)$ is not, collapse of both distributions will only occur if the effects of field-mixing are

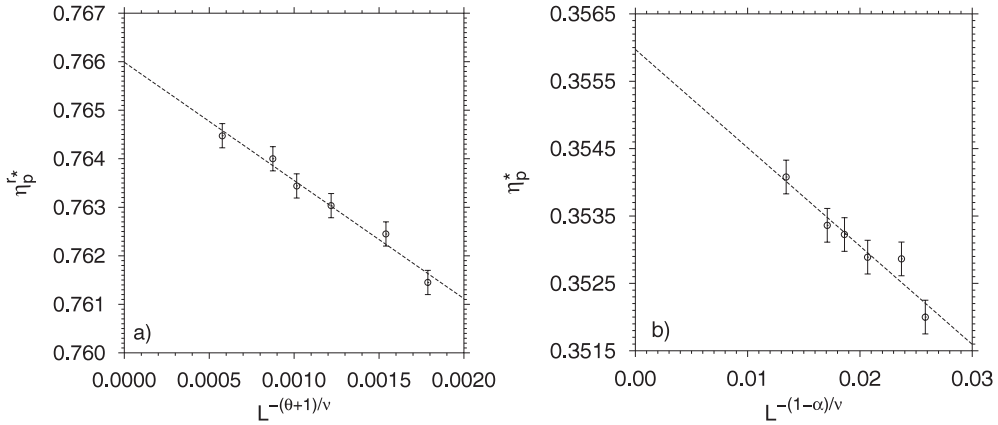

Figure 7. (a) The apparent critical polymer fugacity η_p^{r*} (defined by the collapse criterion described in the text) as a function of $L^{-(\theta+1)/\nu}$. The extrapolation of the linear least-squares fit to infinite volume yields $\eta_{p,cr}^r = 0.766 \pm 0.002$. (b) Polymer packing fraction η_p^* as a function of $L^{-(1-\alpha)/\nu}$. The least-squares fit yields an infinite volume estimate $\eta_{p,cr} = 0.3562 \pm 0.0006$.

properly accounted for. In practice, this is achieved by measuring $P(\eta_c - r\eta_p)$, rather than $P(\eta_c)$ itself [24]. The quantity $P(\eta_c - r\eta_p)$ is defined as the probability of observing the linear combination $\eta_c - r\eta_p$, with r being a system-dependent parameter. For the AO model we found $r \approx 0.25$ by using 'trial and error'. The resulting probability distribution is symmetric and can be mapped onto $P_L(x)$, provided one has accurate data. An example of a collapse is also shown in figure 6 and demonstrates the good quality of our data.

As another method to locate the critical point, we measured η_p^{r*} for a number of different system sizes L. A plot of η_p^{r*} versus $L^{-(\theta+1)/\nu}$ should then lead to a straight line (the values of the critical exponents appropriate to the 3D Ising model are $\theta \approx 0.54$, $\nu \approx 0.629$ and $\alpha = 0.11$). The intercept point of the line with the ordinate equals the critical polymer fugacity, for which we obtain $\eta_{p,cr}^r = 0.766 \pm 0.002$; see figure 7(a). This value is in excellent agreement with the previous estimate.

The remaining critical quantities are determined in a similar way. For each system size L, we record the colloid chemical potential μ_c^*, the colloid packing fraction η_c^*, and the polymer packing fraction η_p^*, at the point where collapse onto the master curve occurs. A plot of μ_c^* as a function of $L^{-(\theta+1)/\nu}$ yields a straight line; this holds also for η_c^* and η_p^* as functions of $L^{-(1-\alpha)/\nu}$. From extrapolation to infinite volume one gets the desired critical quantities which are indicated in figures 7(b) and 8. For completeness, we have also marked the critical point in the phase diagrams, as shown in figure 3.

In summary, our MC method for the AO model combined with FSS allows for accurate estimates of the critical point. Moreover, the quality of the collapse in figure 6, together with the flatter binodal in figure 3, gives evidence that the AO model indeed belongs to the 3D Ising universality class. Although hardly surprising, this result is important because it may explain the discrepancy of the (mean-field) free volume binodal with that estimated from our simulation.

4. Capillary waves

We now focus on the analysis of spatial fluctuations of the interfaces formed between the polymers and the colloids at states in the two-phase region. A consequence of these fluctuations

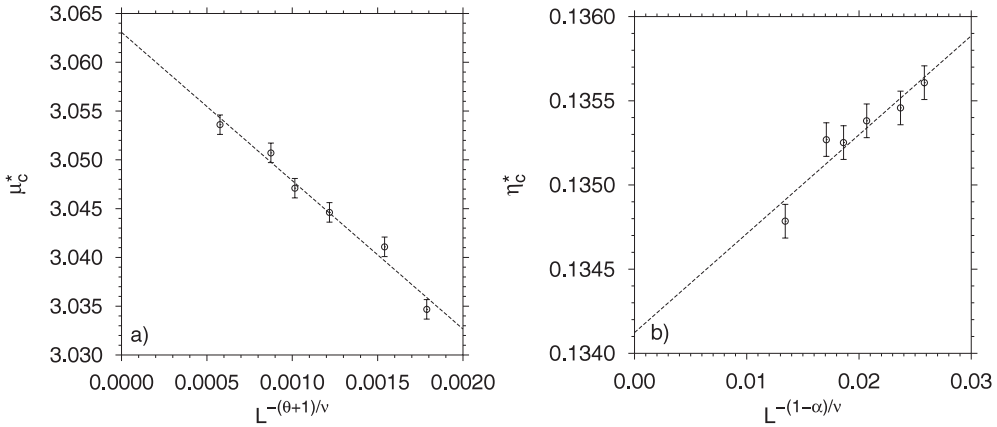

Figure 8. (a) Colloid chemical potential μ_c^* as a function of $L^{-(\theta+1)/\nu}$. The least-squares fit yields an infinite volume estimate $\mu_{c,cr} = 3.063 \pm 0.003$. (b) Colloid packing fraction η_c^* as a function of $L^{-(1-\alpha)/\nu}$. The least-squares fit yields an infinite volume estimate $\eta_{c,cr} = 0.1340 \pm 0.0002$.

is that the colloid–polymer interface does not have a flat shape but it exhibits spontaneous undulations which can be quantified by the mean-square amplitude of the interface thickness around a flat interface. Capillary wave theory [28–31] expresses the free energy cost ΔF_s of the interfacial fluctuations by the interfacial tension γ times the excess in the area of the undulated interface over that of the flat one. Thereby, one assumes that spatial variations of the interface position occur over length scales much larger than the typical width of the interface. If one denotes the local deviation of the interface position $z_0(x, y)$ (z is the Cartesian component perpendicular to the interface, x, y the ones parallel to it) from the mean value by $h(x, y) = z_0(x, y) - \langle z_0(x, y)\rangle$, one can write the free energy cost as [31]

$$\Delta F_s = \frac{\gamma}{2}\int \mathrm{d}x\,\mathrm{d}y\left[\left(\frac{\partial h}{\partial x}\right)^2 + \left(\frac{\partial h}{\partial y}\right)^2\right]. \tag{2}$$

In the derivation of equation (2) one makes the further assumption that the derivatives $\partial h/\partial x$ and $\partial h/\partial y$ are small, i.e. spatial variations of the interface are considered to be slowly varying fluctuations.

$h(\vec{\rho}) \equiv h(x, y)$ can be expressed in Fourier coordinates $h(\rho) = \frac{1}{\sqrt{A}}\sum_{\vec{q}} h(\vec{q})\mathrm{e}^{\mathrm{i}\vec{q}\cdot\vec{\rho}}$ (with the wavevector $\vec{q} = (q_x, q_y)$ and A denoting the area of the flat interface) and then equation (2) can be rewritten as

$$\Delta F_s = \frac{\gamma}{2}\sum_{\vec{q}} q^2|h(\vec{q})|^2. \tag{3}$$

Thus, the different $\vec{q}$ modes are decoupled and one can make use of the equipartition theorem to obtain

$$\langle|h(\vec{q})|^2\rangle = \frac{1}{\gamma q^2}. \tag{4}$$

One can now easily calculate the mean-squared real space fluctuations around a flat profile by

$$w_{cw}^2 = \langle h^2(\vec{\rho})\rangle = \sum_{\vec{q}}\langle|h(\vec{q})|^2\rangle = \frac{1}{(2\pi^2)}\int \mathrm{d}\vec{q}\,\langle|h(\vec{q})|^2\rangle, \tag{5}$$

which leads with equation (4) to

$$w_{cw}^2 = \langle h^2(\vec{\rho})\rangle = \frac{1}{2\pi\gamma}\int_{2\pi/L_x}^{2\pi/a}\frac{\mathrm{d}q}{q} = \frac{1}{2\pi\gamma}\ln\left(\frac{L_x}{a}\right). \tag{6}$$

Here, $L_x = L_y$ is the length of the system in the directions parallel to the interface and a is a cutoff length introduced in accordance with the assumption that only modes with a wavelength larger than the typical width of the interface are taken into account.

In standard mean-field theory an expression for the functional form of the interfacial profile $\phi(z)$ between the phase-separated phases can be given. One yields a hyperbolic tangent of the form

$$\phi(z) = A + B \tanh\left(\frac{z - z_0}{w_0}\right), \tag{7}$$

where A and B are parameters that are related to the bulk densities, z_0 is the position of the interface and w_0 its width. If one wants to combine the mean-field result with that of capillary wave theory, one interprets w_0 as a width of an intrinsic profile that is superposed by fluctuations described by w_{cw}. The total width w of the profile is then obtained from a convolution approximation [32],

$$w^2 = w_0^2 + \frac{\pi}{2} w_{\mathrm{cw}}^2 = w_0^2 + \frac{1}{4\gamma} \ln L - \frac{1}{4\gamma} \ln(a). \tag{8}$$

By means of this equation it is impossible to determine an intrinsic width w_0 from experimental or simulation data since one cannot disentangle the intrinsic width contribution w_0^2 from the 'cut-off' contribution $-\frac{1}{4\gamma} \ln(a)$. Thus, one cannot compare directly the interfacial profiles as obtained from the simulation to a mean-field result as the one by Vrij [33] or the one by Brader and Evans [34] for the AO model. This issue has been studied in detail for the case of polymer mixtures in [35–39].

The main issue in the following is to investigate whether a logarithmic divergence as described by equation (8) can be seen in the simulation of the AO model. To this end, we restrict the simulation to a region inside the phase-separated regime of the phase diagram for $q = 0.8$ (see figure 3). In this work we study states at $\eta_{\mathrm{c}} = 0.13$ for the three polymer reservoir packing fractions $\eta_{\mathrm{p}}^r = 0.9$, 1.0, and 1.1. As can be inferred from figure 3, these state points are well inside the phase-separated regime. The simulations are performed in a box with dimensions $V = L_x \times L_y \times L_z$ using periodic boundary conditions. To obtain the desired colloid packing fraction, the number of colloids inside V is $N_{\mathrm{c}} = \eta_{\mathrm{c}} V / V_{\mathrm{c}}$, with $V_{\mathrm{c}} = (4\pi/3) R_{\mathrm{c}}^3$ being the volume of a single colloid. To start the simulations, we prepare a box with N_{c} randomly inserted colloids. We then equilibrate this system with grand canonical cluster moves and random particle displacements. During equilibration, polymers enter the simulation volume via the grand canonical cluster moves [15, 16]. Cluster moves and displacements are attempted in a 1:1 ratio. Additionally, we restrict the grand canonical moves such that the number of colloids ranges between N_{c} and $N_{\mathrm{c}} + 1$ inclusive. We continue to equilibrate until phase separation has occurred and a colloid–polymer interface has formed. A snapshot of the result of this procedure is shown in figure 9.

To obtain the colloid density profile, we measure the local colloid packing fraction $\phi(z)$ along the L_z axis after having shifted the centre of mass of the colloid phase to the origin. In the following, $L_x = L_y$ and $L_z > L_x$ such that the colloid–polymer interface is always perpendicular to L_z. To improve statistics, we average $\phi(z)$ approximately every 500 attempted MC moves per particle. The total number of averages taken is typically 10^4. Examples of such averaged profiles at different η_{p}^r are shown in figure 10. The solid curves in this figure are fits with the mean-field formula, equation (7). As demonstrated in figure 10, this formula describes the simulation data very well at the considered state points away from the critical point. However, the interfacial width that we read off from the fits with equation (7) is not the intrinsic width w_0 but it should be described by the one given by equation (8) if capillary wave theory is applicable. Therefore, we identify the parameter w_0 in equation (8) by the width w

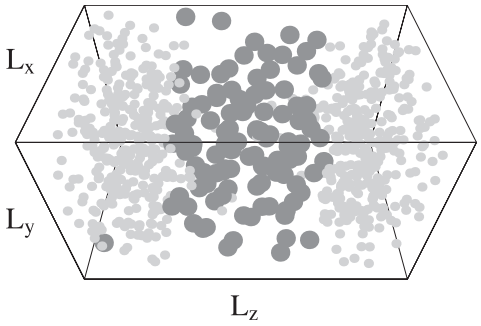

Figure 9. Typical snapshot of a phase-separated AO mixture obtained using our simulation method. The mixture is contained in a box with dimensions $L_x \times L_y \times L_z$ and periodic boundary conditions in all directions. The dark spheres are colloidal particles, light spheres are polymers.

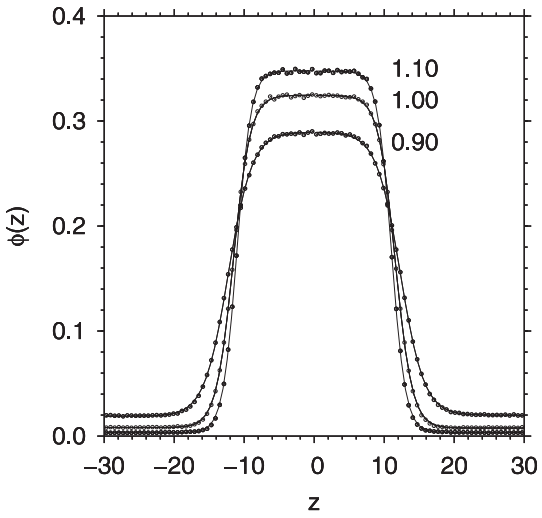

Figure 10. Local colloid packing fraction $\phi(z)$ along the L_z axis in a phase-separated AO model with $q = 0.8$ and several values of η_p^r as indicated. The simulations were performed in a box with dimensions $L_x = L_y = 20$ and $L_z = 60$ using periodic boundary conditions. Open circles are simulation data; the solid curves are fits using the hyperbolic tangent of equation (7).

and we discuss in detail the dependence of w on a variation of $L \equiv L_x = L_y$ and $D \equiv L_z$, i.e. the size of the simulation box parallel and perpendicular to the interfaces, respectively. Note that we consider only the state with $\eta_p^r = 1.1$ in the following.

Consider again the snapshot in figure 9. Since we use periodic boundary conditions in all directions, the phase-separated mixture contains two interfaces as a result. If the perpendicular dimension D is small, the interfaces will interact with each other. It is not surprising then for the interfacial width w to be D dependent. However, one would expect that if D becomes large enough, any L dependence in w should vanish. This is indeed the case, provided the lateral dimension L is sufficiently large. If L is (too) small, the interfacial width will show a systematic D dependence that, moreover, depends on the simulation ensemble. In the grand canonical ensemble, one expects a (roughly) linear dependence of w on D. In this case, the dominant fluctuations of the interface are those where the interface fluctuates as a whole. For large D, the interface is freely fluctuating, and thus displacements of order D can occur. In

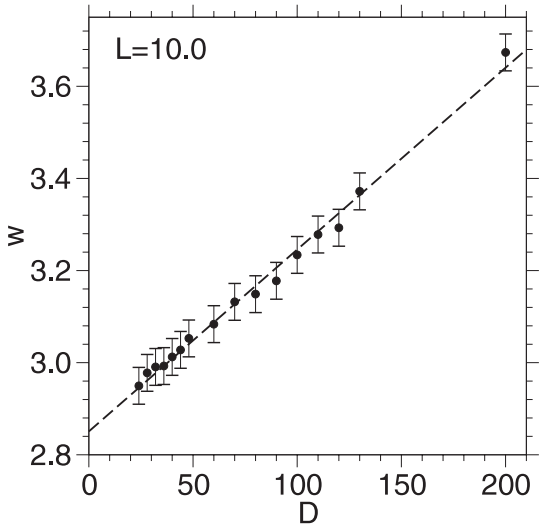

Figure 11. Interfacial width w as a function of the perpendicular box dimension D for an AO mixture with lateral box dimensions $L = 10$. For small lateral dimensions in the grand canonical ensemble, the interfacial width grows roughly linearly with D, indefinitely (the dashed line is a fit with a linear law).

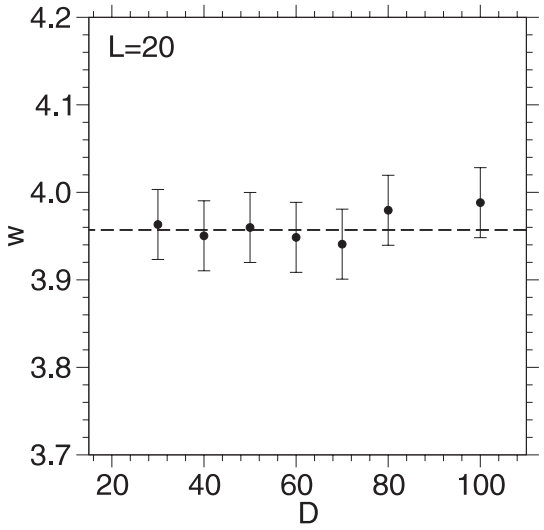

Figure 12. Interfacial width w as a function of the perpendicular box dimension D for an AO mixture with lateral box dimensions $L = 20$. In this case, the lateral dimension is sufficiently large for any D dependence to vanish.

figure 11, the linear dependence of w on D is confirmed for the AO model. For our AO mixture with $q = 0.8$, linear growth is observed for $L \approx 10$ and smaller.

It is thus important to choose L large enough such that the interfacial width does not depend on D any more. This needs to be checked by varying D over a large range. For the AO model, we find such a regime for $L \approx 20$ and higher; see figure 12. Once this regime is established, we vary the lateral dimension L to study its effect on w. In this regime the

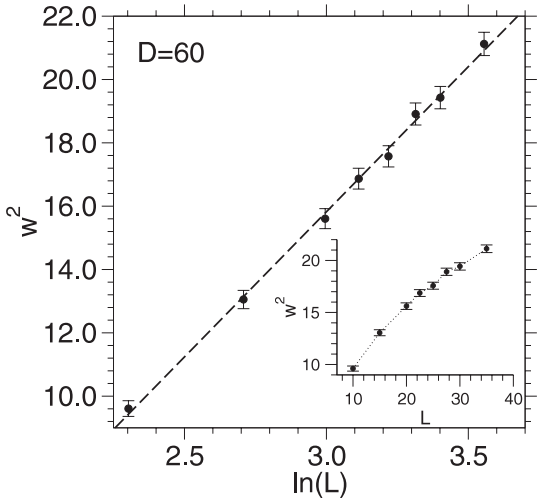

Figure 13. Interfacial width squared w^2 as a function of the lateral dimension L for a phase-separated AO model with $D = 60$. In this regime the logarithmic growth of the interface due to capillary waves is visible (note the logarithmic L scale). The line is a least-squares fit through the simulation data of the form $w^2 = A\ln(L) + B$ (where A and B are fit parameters). The inset shows the same data, but now w^2 is plotted as a function of L to show that the data cannot be described by a linear growth of w^2.

prediction of capillary wave theory, equation (8), can be tested to see whether the square of the interfacial width is proportional to the logarithm of the lateral dimension L. The measured behaviour for the AO model shown in figure 13 is in agreement with this prediction. However, one may argue that the range that is spanned in $\ln L$ is relatively small and that one would obtain also a straight line on a linear L-scale. But, as is demonstrated by the inset of figure 13, the data are not consistent with a linear growth of w^2 with L.

Our results thus confirm the expected dependence of the interfacial width on the perpendicular and lateral dimensions of the simulation volume. As far as simulations are concerned, it is important to establish a regime in which the linear broadening shown in figure 11 has vanished. For an AO model with $q = 0.8$, a lateral dimension of about 20 colloid radii is sufficient to achieve this. In this regime, the expected logarithmic broadening due to capillary waves is confirmed in figure 13. This result is important because it shows that the interfacial width cannot be regarded as an intrinsic variable. Consequently, investigations of the colloid–polymer interface in which these size effects are not addressed must be treated with some care (see also [35] and references therein).

5. Conclusions

In this paper we have used grand canonical MC methods to study the bulk phase behaviour of the AO model. Our results agree qualitatively with previous work, namely that phase separation occurs provided that the polymer fugacity is high enough. However, deviations from mean-field behaviour are clearly visible. We have also determined the interfacial tension of the colloid–polymer interface. Our results confirm the sharp increase in the interfacial tension predicted by DFT. This shows that the AO model is not realistic enough to facilitate comparisons to experiment. We used FSS to accurately determine the critical point. This also provides additional evidence that the AO model indeed belongs to the 3D Ising universality class. Finally, we quantified the effects of the size of the simulation volume on the width of

the colloid–polymer interface due to capillary waves. These effects are not artefacts of the simulation but occur in real systems also [36]. Our results confirm the conclusion of [35], namely that the intrinsic width w_0 of equation (7) is a hypothetical quantity, neither accessible in simulations, nor in experiments.

Acknowledgments

We are grateful to the Deutsche Forschungsgemeinschaft (DFG) for support (TR6/A5) and to K Binder, M Müller, P Virnau, and M Schmidt for stimulating discussion. One of us (JH) was supported by the Emmy Noether programme of the DFG, grants No HO 2231/2–1 and HO 2231/2–2.

References

[1] de Hoog E H A and Lekkerkerker H N W 1999 *J. Phys. Chem.* B **103** 5274
[2] Chen B-H, Payandeh B and Robert M 2000 *Phys. Rev.* E **62** 2369
[3] de Hoog E H A, Lekkerkerker H N W, Schulz J and Findenegg G H 1999 *J. Phys. Chem.* B **103** 10657
[4] Aarts D G A L, Schmidt M and Lekkerkerker H N W 2004 *Science* at press
[5] Asakura S and Oosawa F 1954 *J. Chem. Phys.* **22** 1255
[6] Vrij A 1976 *Pure Appl. Chem.* **48** 471
[7] Lekkerkerker H, Poon W, Pusey P, Stroobants A and Warren P 1992 *Europhys. Lett.* **20** 559
[8] Aarts D, Tuiner R and Lekkerkerker H 2002 *J. Phys.: Condens. Matter* **14** 7551
[9] Schmidt M, Löwen H, Brader J M and Evans R 2000 *Phys. Rev. Lett.* **85** 1934
[10] Brader J M, Evans R, Schmidt M and Löwen H 2002 *J. Phys.: Condens. Matter* **14** L1
[11] Meijer E and Frenkel D 1994 *J. Chem. Phys.* **100** 6873
[12] Bolhuis P, Louis A and Hansen J 2002 *Phys. Rev. Lett.* **89** 128302
[13] Schmidt M, Fortini A and Dijkstra M 2003 *J. Phys.: Condens. Matter* **15** S3411–S3420
[14] Dijkstra M and van Roij R 2002 *Phys. Rev. Lett.* **89** 208303
[15] Vink R L C and Horbach J 2004 submitted
(Vink R L C and Horbach J 2003 *Preprint* cond-mat/0310404)
[16] Vink R L C 2004 *Computer Simulation Studies in Condensed Matter Physics* vol 17, ed D Landau, S Lewis and H Schüttler (Berlin: Springer)
[17] Brader J M, Evans R and Schmidt M 2003 *Mol. Phys.* **101** 3349
[18] Landau D P and Binder K 2000 *A Guide to Monte Carlo Simulations in Statistical Physics* (Cambridge: Cambridge University Press)
[19] Wilding N 2001 *Am. J. Phys.* **69** 1147
[20] Virnau P and Müller M 2004 *J. Chem. Phys.* at press
(Virnau P and Müller M 2003 *Preprint* cond-mat/0306678)
[21] Binder K 1982 *Phys. Rev.* A **25** 1699
[22] Luijten E and Binder K 2001 *Phys. Rep.* **344** 179
[23] Schmidt M 2004 private communication
[24] Wilding N 1996 *Annual Reviews of Computational Physics* vol 4 (Singapore: World Scientific) p 37
[25] Binder K 1981 *Z. Phys.* B **43** 119
[26] Sengers J and Levelt Sengers J 1986 *Annu. Rev. Phys. Chem.* **37** 189
[27] Hilfer R and Wilding N 1995 *J. Phys. A: Math. Gen.* **28** L281
[28] Rowlinson J S and Widom B 1982 *Molecular Theory of Capillarity* (Oxford: Clarendon)
[29] Weeks J D 1977 *J. Chem. Phys.* **67** 3106
[30] Buff F P, Lovett R A and Stillinger F H 1965 *Phys. Rev. Lett.* **15** 621
[31] Safran S A 1994 *Statistical Thermodynamics of Surfaces, Interfaces, and Membranes* (Reading, MA: Addison-Wesley)
[32] Jasnow D 1984 *Rep. Prog. Phys.* **47** 1059
[33] Vrij A 1997 *Physica* A **235** 120
[34] Brader J M and Evans R 2000 *Europhys. Lett.* **49** 678
[35] Binder K and Müller M 2000 *Int. J. Mod. Phys.* C **11** 1093
[36] Kerle T, Klein J and Binder K 1999 *Eur. Phys. J.* B **7** 401
[37] Werner A, Schmid F, Müller M and Binder K 1997 *J. Chem. Phys.* **107** 8175
[38] Werner A, Müller M, Schmid F and Binder K 1999 *J. Chem. Phys.* **110** 1221
[39] Werner A, Schmid F, Müller M and Binder K 1999 *Phys. Rev.* E **59** 728